Introduction to Control (034040)

Tutorial 12

Question 1. Consider the one-dimensional heat propagation in a semi-infinite rod studied in Tutorial 10, where the control signal is the temperature u at one end and that the output is the temperature y_x at a point along the rod at distance $x > 0$ [m] from the end. The transfer function of this system is

$$P_x(s) = \mathrm{e}^{-a_x\sqrt{s}}, \quad \text{where } a_x := \frac{x}{\sqrt{\alpha}} > 0 \tag{1}$$

where $\alpha > 0$ [m^2/s] is the rod thermal diffusivity. We assume that at $t < 0$ the system is in its equilibrium with $u(t) = y_x(t) = 20°\mathrm{C}$.

1. What K_u and T_u are produced by the Ziegler-Nichols closed-loop experiment ?
2. Design a P controller by the Ziegler-Nichols table. Analyze the resulting stability margins. Then, assuming that $\alpha = 1.27 \cdot 10^{-4}$ [m^2/s] (corresponds to a golden rod) and $x = 0.1$ [m], simulate the system response to the step reference change from 20° to 30° at $t = 0$, i.e. $r = 20 + 10 \cdot \mathbb{1}$ and the step disturbance $d = \mathbb{S}_{-120}\mathbb{1}$, which may reflect a failure in the actuator (heater) at $t = 2$ [min].
3. Under the same conditions, design a PI controller, analyze it, and simulate its response under the unity-feedback implementation scheme presented in Fig. 1(a). Compare the response with that under the implementation scheme presented in Fig. 1(b).
4. Under the same conditions, design a PID controller, analyze it, and simulate its response under the unity-feedback implementation scheme presented in Fig. 1(a). Compare the response with that under the implementation scheme presented in Fig. 1(b).

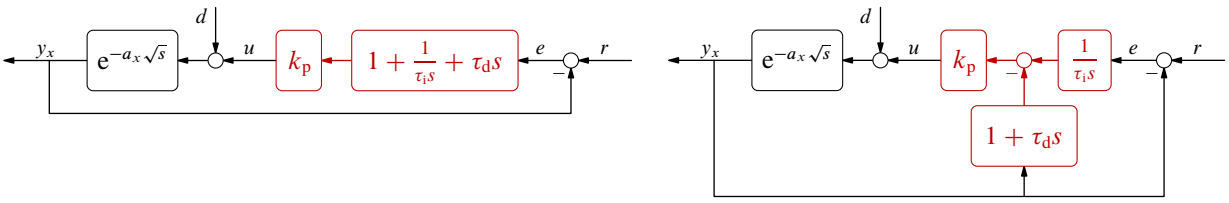

(a) Unity-feedback implementation

(b) Alternative feedback implementation (PI or PID)

Fig. 1: Closed-loop temperature control in a semi-infinite rod

Solution.

1. The frequency response in this case (remember Tutorial 10) is

$$P_x(\mathrm{j}\omega) = \mathrm{e}^{-a_x\sqrt{\omega/2}}\,\mathrm{e}^{-\mathrm{j}a_x\sqrt{\omega/2}}.$$

Its polar plot is presented in Fig. 2(a). Important parameters for the Ziegler-Nichols experiment are its phase crossover frequency and the corresponding gain, i.e.

$$\omega_\phi = \frac{2\pi^2}{a_x^2} \quad \text{and} \quad |P_x(\mathrm{j}\omega_\phi)| = \mathrm{e}^{-\pi}.$$

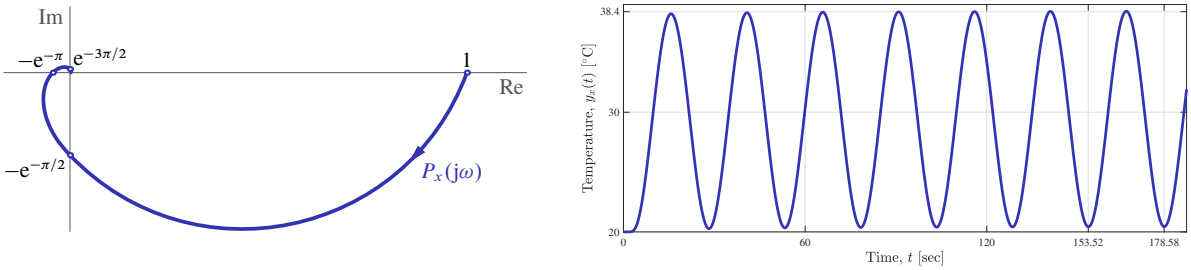

(a) Polar plot

(b) Step response

Fig. 2: Ziegler-Nichols experiment for $P_x(s)$ in Question 1 (here $a_x = 8.8736$)

This immediately yields

$$K_u = \frac{1}{|P_x(j\omega_\phi)|} = e^\pi \approx 23.1407 \quad \text{and} \quad T_u = \frac{2\pi}{\omega_\phi} = \frac{a_x^2}{\pi} = \frac{x^2}{\alpha\pi}.$$

This K_u is independent of the system parameters, whereas T_u does depend on them. The step response in the Ziegler-Nichols experiment is presented in Fig. 2(b). It can be seen that the response oscillates with a period of about 25.06[sec], which corresponds to the T_u above under $a_x = 8.8736$.

2. It follows from Table 1 that the tuned P controller is

	k_p	τ_i	τ_d
P	$0.5\,K_u$		
PI	$0.45\,K_u$	$\frac{5}{6}T_u$	
PID	$0.6\,K_u$	$0.5T_u$	$0.125T_u$

Table 1: Ziegler-Nichols table

$$C_\mathrm{p}(s) = \frac{e^\pi}{2} \approx 11.5703.$$

It yields $\mu_\mathrm{g} = 2$, by construction. The crossover frequency in this loop satisfies

$$\frac{e^\pi}{2} e^{-a_x\sqrt{\omega_\mathrm{c}/2}} = 1 \iff \omega_\mathrm{c} = \frac{2(\pi - \ln 2)^2}{a_x^2} \approx \frac{11.99}{a_x^2},$$

which is a decreasing function of x and an increasing function of α. Therefore,

$$\mu_\mathrm{ph} = \pi - \ln\frac{e^\pi}{2} = \ln 2 \approx 0.69\,[\mathrm{rad}] \approx 39.7^\circ,$$

is independent of system parameters. The delay margin does depend on them, as

$$\mu_\mathrm{d} = \frac{\mu_\mathrm{ph}}{\omega_\mathrm{c}} = \frac{a_x^2 \ln 2}{2(\pi - \ln 2)^2} \approx 0.0578\,a_x^2$$

is an increasing (decreasing) function of x (α).

The response of this controller under the given thermal diffusivity at the distance of 10 [cm] from the end to step reference and disturbance signals is presented in Fig. 3 (note that the time axis is in minutes). The crossover frequency in this case if $\omega_\mathrm{c} \approx 0.1523$ [rad/sec] and the resulted closed-loop

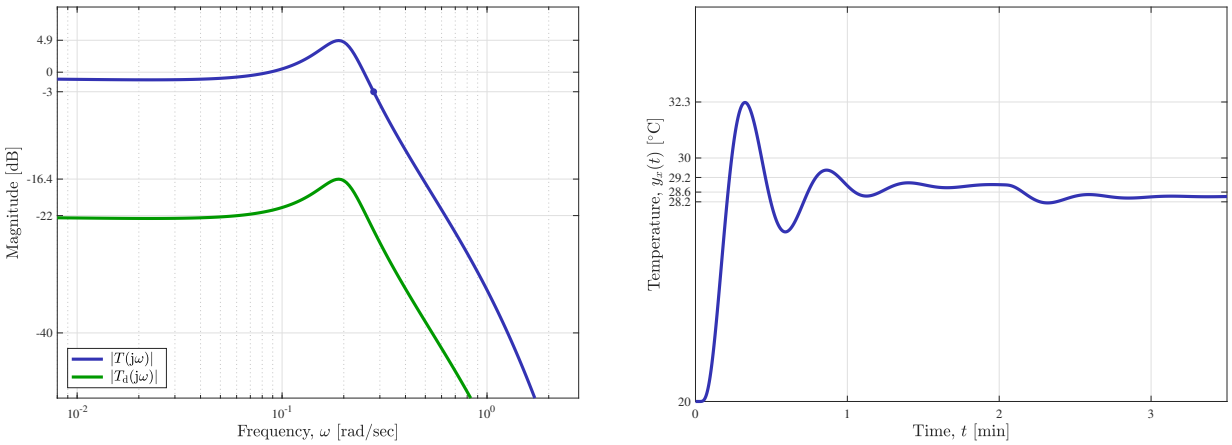

(a) Closed-loop frequency responses

(b) Time response

Fig. 3: Closed-loop responses, P controller

bandwidth is $\omega_b \approx 0.28$ [rad/sec]. The resonant peak in the complementary sensitivity frequency response gives rise to an overshoot of about 34% (steady-state deviation from the initial equilibrium temperature is 9.2, the peak deviation from it is 12.3). The disturbance sensitivity, presented by the green line in Fig. 3(a), is quite small, with its peak at -16.4 [dB]. This can be seen in the time response, where the step disturbance at $t = 2$ [min] has relatively limited effect on the time response. Note that the steady-state errors are not zero, because the loop contains no integrators.

3. Referring again to Table 1, the PI controller tuned according to Ziegler-Nichols rules is

$$C_{PI}(s) = 0.45e^{\pi}\left(1 + \frac{1.2\pi}{a_x^2 s}\right) \approx \frac{10.4133(s + 0.04788)}{s}.$$

Stability margins, as well as the corresponding crossover frequencies, can no longer be calculated analytically. For example, the phase crossover frequency should now satisfy

$$-a_x\sqrt{\frac{\omega_\phi}{2}} - \frac{\pi}{2} + \arctan\frac{a_x^2\omega_\phi}{1.2\pi} = -\pi \iff a_x\sqrt{\frac{\omega_\phi}{2}} - \arctan\frac{a_x^2\omega_\phi}{1.2\pi} = \frac{\pi}{2},$$

which is a transcendental equation having no closed-form solution (although we know that the solution is unique). Its numerical solution in the case of a golden rod at distance 10 [cm] from the rod end, where $a_x \approx 8.8736$, yields $\omega_\phi \approx 0.2173$ [rad/sec], which is a slight decrease with respect to that in the P-controller case (it was $\omega_\phi \approx 0.2507$ [rad/sec] there). Hence, we determine all required quantities from the Bode plot of the loop $L_{PI}(s) = P_x(s)C_{PI}(s)$ presented in Fig. 4(a). We can see that

$$\mu_g \approx 4.8\,[\text{dB}] \approx 1.7469 \quad \text{and} \quad \mu_{ph} \approx 25°,$$

with $\omega_c \approx 0.1456$ [rad/sec] (about the same as with C_P). These stability margins happen to be smaller than the corresponding margins under the P controller C_P. The polar plot in the PI case, presented in Fig. 4(b) by the blue line, is also generally closer to the critical point than the loop under the P controller (green dashed line). Consequently, the closed-loop complementary sensitivity magnitude exhibits a larger resonant peak (the blue line in Fig. 4(c)) than the corresponding plot in Fig. 3(a). This, in turn, gives rise to a larger overshoot (about 59% in Fig. 4(d) vs. 34% in the P case in Fig. 3(b)). The resulted closed-loop bandwidth, $\omega_b \approx 0.26$ [rad/sec], is close to that in the previous item. The disturbance sensitivity (the green line in Fig. 4(c)) has a slightly larger peak that that in Fig. 3(a), but

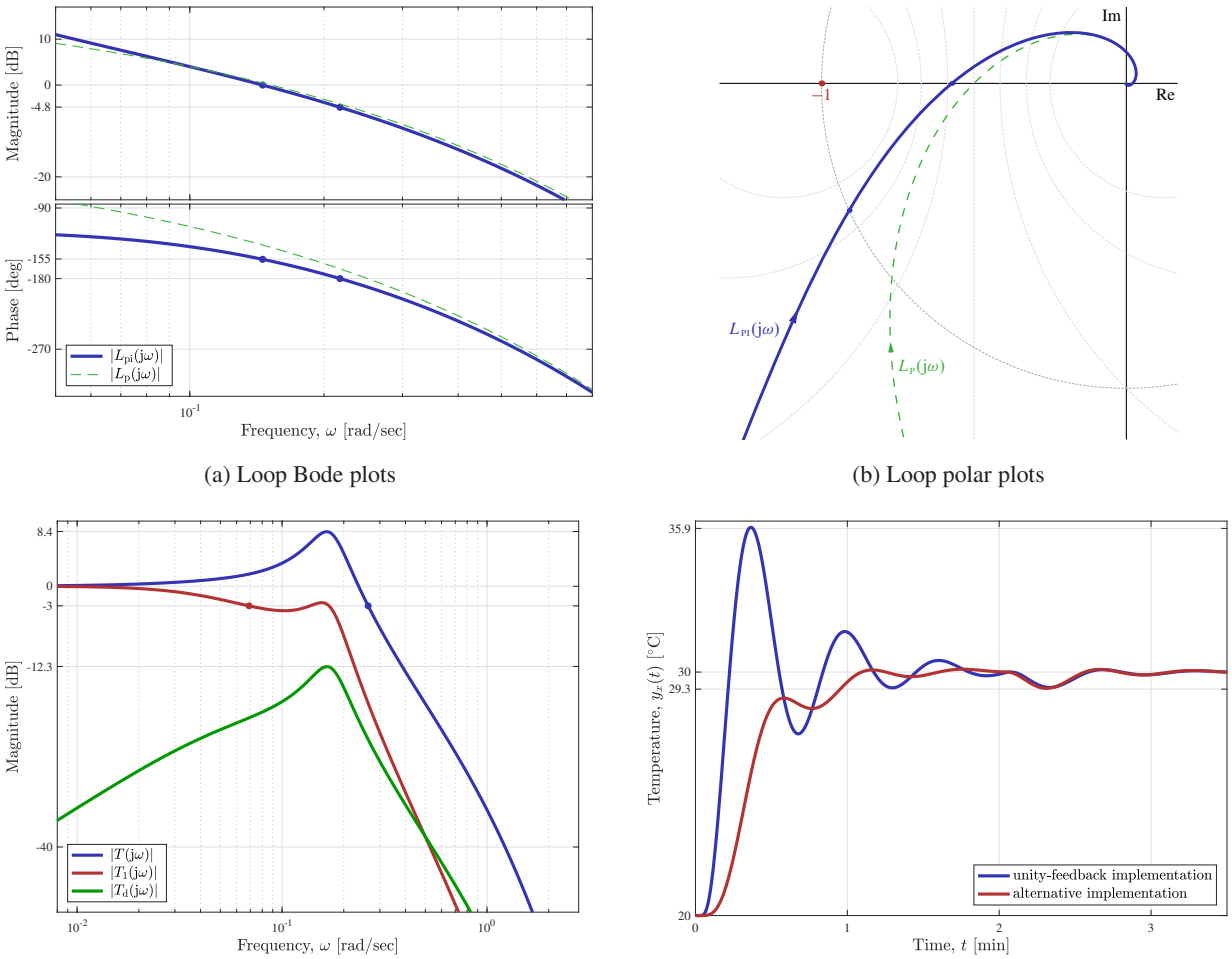

(a) Loop Bode plots

(b) Loop polar plots

(c) Closed-loop frequency responses

(d) Time response

Fig. 4: Closed-loop responses, PI controller

substantially lower gain in low frequencies. In particular, the static gain of T_d is now zero, which gives rise to a zero steady-state error to a step in d.

The command response can be improved if C_PI is implemented in via the scheme in Fig. 1(b). The disturbance sensitivity then remains unchanged, whereas the system $r \mapsto y_x$,

$$T_1(s) = T_\mathrm{d}(s)\frac{k_\mathrm{p}}{\tau_\mathrm{i}\, s} = \frac{k_\mathrm{p}\, \mathrm{e}^{-a_x\sqrt{s}}}{\tau_\mathrm{i}\, s + k_\mathrm{p}\, \mathrm{e}^{-a_x\sqrt{s}}(\tau_\mathrm{i}\, s + 1)} \neq \frac{k_\mathrm{p}\, \mathrm{e}^{-a_x\sqrt{s}}(\tau_\mathrm{i}\, s + 1)}{\tau_\mathrm{i}\, s + k_\mathrm{p}\, \mathrm{e}^{-a_x\sqrt{s}}(\tau_\mathrm{i}\, s + 1)} = T(s).$$

Specifically, $T_1(s)$ does not have the zero at $s = -1/\tau_\mathrm{i}$, which contributes to the increase of the resonant peak of T. Indeed, $|T_1(\mathrm{j}\omega)|$, shown by the red line in Fig. 4(c), has a substantially lower peak. It alwo has a lower bandwidth, $\omega_\mathrm{b} \approx 0.069$ [rad/sec], although in this case that might be misleading[1]. The step response, shown by the red line in Fig. 4(d), boasts a substantially lower overshoot in the response to a step in r (the response at $t < 2$ [min]). At the same time, the response to d should be the same in both configurations. This is not completely so for the responses in Fig. 4(d). The difference there, however, is caused by the fact that the command responses are not in their steady state yet at $t = 2$ [min], when the disturbance is applied.

[1] If we measured the bandwidth at the -3.8 dB level, it would increase by more than a factor of 2.5, to $\omega \approx 0.177$ [rad/sec].

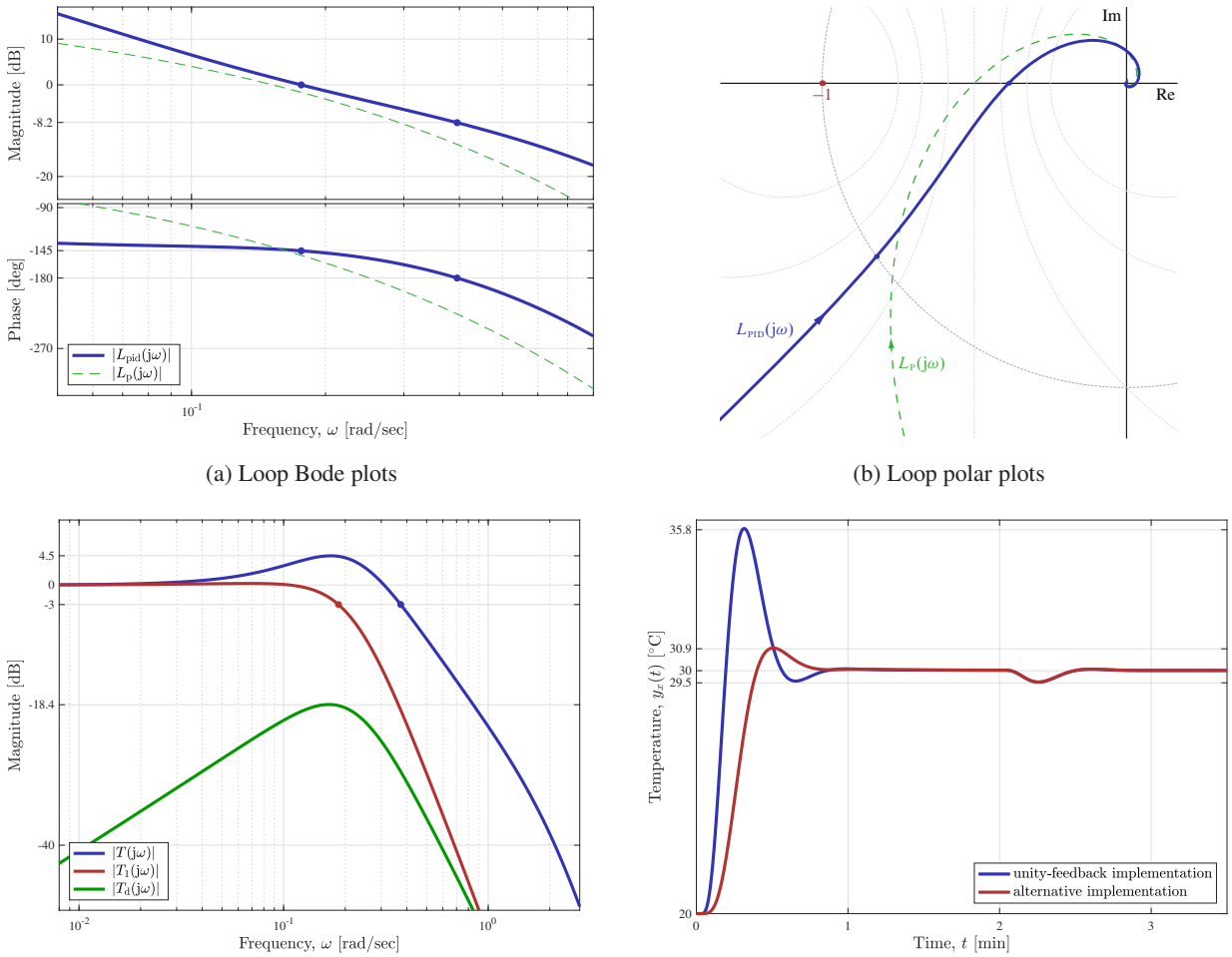

(a) Loop Bode plots

(b) Loop polar plots

(c) Closed-loop frequency responses

(d) Time response

Fig. 5: Closed-loop responses, PID controller

4. The PID controller tuned according to Table 1 is

$$C_{\text{PID}}(s) = \frac{3\text{e}^{\pi}}{5}\left(1 + \frac{2\pi}{a_x^2\, s} + \frac{a_x^2}{8\pi}\, s\right) = \frac{3\text{e}^{\pi} a_x^2}{40\pi} \cdot \frac{(s + 4\pi/a_x^2)^2}{s} = \frac{43.5(s + 0.1596)^2}{s}$$

(a PID controller tuned by Table 1 always has a double zero at $s = -1/\sqrt{\tau_{\text{i}}\tau_{\text{d}}} = -4/T_u$, perhaps aesthetic appeal was a criterion for J. G. Ziegler and N. B. Nichols). The Bode plot of the resulted loop is depicted in Fig. 5(a) by the blue line. The stability margins are

$$\mu_{\text{g}} \approx 8.2\,[\text{dB}] \approx 2.58 \quad \text{and} \quad \mu_{\text{ph}} \approx 35^{\circ},$$

which is better than the margins that we had in the PI case (the corresponding $\omega_\phi \approx 0.4\,[\text{rad/sec}]$ and $\omega_{\text{c}} \approx 0.18\,[\text{rad/sec}]$ are close to what we had in the P and PI cases). As a result, the polar plot, Fig. 5(b), is now further from the critical point, which results in a lower peak in the complementary sensitivity frequency response (Fig. 5(c)). The step response (Fig. 5(d), blue line) still has a high overshoot, more than 50%, but now the response is substantially less oscillatory (this can be expected by noting that the blue peak in Fig. 5(c) is noticeable "wider" than that in Fig. 4(c)). The settling times, under a settling level of 1%, is now below 50 [sec], which is substantially below of what we had in the P and PI cases.

The command response can, again, be improved by implementing the PID controller in the form presented in Fig. 1(b). This implementation eliminates the double zero at $s = -4\pi/a_x^2 \approx 0.16$ from the transfer function connecting r and y_x, which was the reason for the non-oscillating overshoot of the command response. In this implementation the system $T_1 : r \mapsto y_x$,

$$T_1(s) = T_\mathrm{d}(s)\frac{k_\mathrm{p}}{\tau_\mathrm{i}\, s} = \frac{k_\mathrm{p}\, \mathrm{e}^{-a_x\sqrt{s}}}{\tau_\mathrm{i}\, s + k_\mathrm{p}\, \mathrm{e}^{-a_x\sqrt{s}}(\sqrt{\tau_\mathrm{i}\tau_\mathrm{d}}\, s + 1)^2} \neq \frac{k_\mathrm{p}\, \mathrm{e}^{-a_x\sqrt{s}}(\sqrt{\tau_\mathrm{i}\tau_\mathrm{d}}\, s + 1)^2}{\tau_\mathrm{i}\, s + k_\mathrm{p}\, \mathrm{e}^{-a_x\sqrt{s}}(\sqrt{\tau_\mathrm{i}\tau_\mathrm{d}}\, s + 1)^2} = T(s),$$

has no zeros, which results in a monotonically decreasing frequency response, see the red line in Fig. 5(c). The command, presented by the red line in Fig. 5(d), response has then a much lower overshoot, about 9%. The disturbance responses under both implementations are expectably identical.

It should be emphasized that all responses presented above were taken at the very same point, located 10 [cm] from the rod end, where the temperature was measured. The closed-loop transfer function from the reference signal to the temperature at a point located z [m] from the rod end is

$$T_1(s) = \frac{Y_z(s)}{R(s)} = \frac{Y_z(s)/U(s)}{Y_x(s)/U(s)}\frac{Y_x(s)}{R(s)} = \frac{\mathrm{e}^{-a_z\sqrt{s}}}{\mathrm{e}^{-a_x\sqrt{s}}}\frac{Y_x(s)}{R(s)} = \frac{k_\mathrm{p}\, \mathrm{e}^{-a_z\sqrt{s}}}{\tau_\mathrm{i}\, s + k_\mathrm{p}\, \mathrm{e}^{-a_x\sqrt{s}}(\sqrt{\tau_\mathrm{i}\tau_\mathrm{d}}\, s + 1)^2}.$$

Its step responses for $z \in \{5, 8.75, 11.25, 15, 20\}$ [cm] are presented in Fig. 6. We can see that the further we

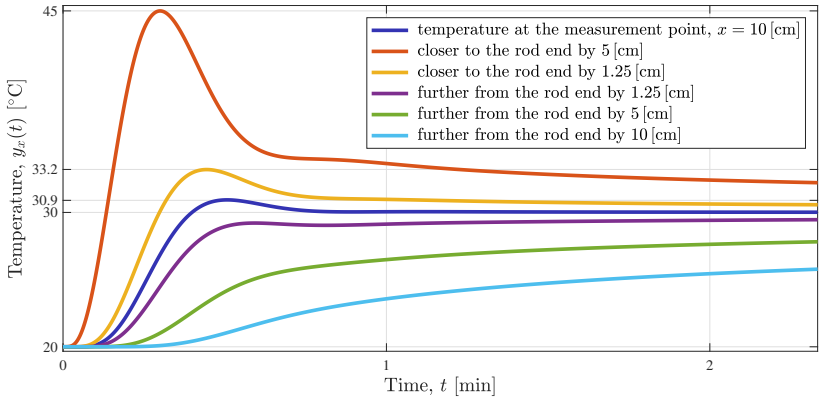

Fig. 6: Temperature along the rod under the PID controller designed in item 4

deviate from the measurement point, the further we deviate from the tuned behavior. As we move closer to the actuation point, the response overshoots, whereas as we move further from the actuation point, the response becomes slower. This behavior suggests that controlling the temperature over a spatially distributed media requires more than one lumped actuator ... ▽

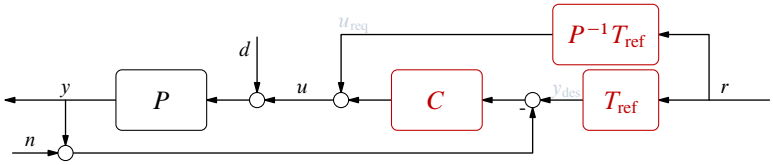

Fig. 7: 2DOF control configuration for the system in Question 2

Question 2. Consider a system consisting of a plant and a feedback controller given by their transfer functions

$$P(s) = \frac{750}{s(s+5)(s+10)} \quad \text{and} \quad C(s) = 2.9303\left(\frac{1.8455s + 11.5}{s + 21.2228}\right)^2 \frac{10s + 11.5}{10s + 0.0989},$$

respectively. When implemented in the unity-feedback architecture, this system was studied in Tutorial 11 (the second design in Question 1) and has a closed-loop bandwidth of about 20 [rad/sec], a phase margin of 35°, and steady-state error to a step disturbance of 1% of the disturbance magnitude. The transient command response for this system was not quite exciting, with an overshoot of 42% and a settling time of 1.84 [sec] under settling level 1% (we could have expected shorter transients for this bandwidth).

To improve the command response, consider the use of the 2DOF configuration in Fig. 7, where the reference model T_{ref} is stable and such that $C_{\text{ol}} = P^{-1}T_{\text{ref}}$ is stable as well.

1. Derive the relation between the exogenous signals r, d, and n and the signals of interest y and u.

2. Choose a reference model of the form

$$T_{\text{ref}}(s) = \frac{1}{(\tau s + 1)^n}$$

having the minimum possible degree n and such that the high-frequency gain of the system $r \mapsto u$ is the same as the high-frequency gain of the control sensitivity, $T_{\text{c}}(\infty)$. Simulate the system with $r = \mathbb{1}$ and $d = -0.2\$_{-1.84}\mathbb{1}$. Compare the results with those obtained for the unity-feedback (1DOF) implementation of the control system.

3. Suggest an admissible reference model T_{ref}, which has $T_{\text{ref}}(0) = 1$, satisfies the requirements of the previous item, and renders the block $P^{-1}T_{\text{ref}}$ simplest (i.e. results in its lowest possible degree), which simplifies its implementation. Simulate the resulting closed-loop system.

Solution.

1. There are many ways to do that. Consider a purely algebraic one. To this end, write

$$u = u_{\text{req}} + C(y_{\text{des}} - y - n) = P^{-1}T_{\text{ref}}\, r + C(T_{\text{ref}}r - Pd - Pu - n)$$

Hence, in the Laplace transform domain

$$(1 + P(s)C(s))U(s) = \frac{T_{\text{ref}}(s)(1 + P(s)C(s))}{P(s)}R(s) - P(s)C(s)D(s) - C(s)N(s)$$

or, equivalently,

$$U(s) = \frac{T_{\text{ref}}(s)}{P(s)}R(s) - \overbrace{\frac{P(s)C(s)}{1 + P(s)C(s)}}^{T(s)}D(s) - \overbrace{\frac{C(s)}{1 + P(s)C(s)}}^{T_{\text{c}}(s)}N(s).$$

The output y satisfies then

$$Y(s) = P(s)U(s) + P(s)D(s) = T_{\text{ref}}(s)R(s) + \overbrace{\frac{P(s)}{1+P(s)C(s)}}^{T_{\text{d}}(s)}D(s) - \frac{P(s)C(s)}{1+P(s)C(s)}N(s).$$

It is worth emphasizing that T, T_{d}, and T_{c} are the very familiar closed-loop systems for the unity-feedback architecture.

2. Because $P(s)$ is a minimum-phase transfer function, the only limitation on $T_{\text{ref}}(s)$ is that its pole excess is at least 3. Hence, the smallest admissible $n = 3$.

   Now, the high-frequency gain of the control sensitivity is

   $$T_{\text{c}}(\infty) = \frac{C(\infty)}{1+P(\infty)C(\infty)} = C(\infty) \approx 10.$$

   With $n = 3$, the high-frequency gain of

   $$C_{\text{ol}}(s) = \frac{T_{\text{ref}}(s)}{P(s)} = \frac{s(s+5)(s+10)}{750(\tau s+1)^3}$$

   is $C_{\text{ol}}(\infty) = 1/(750\tau^3)$. Hence, the time constant at which $C_{\text{ol}}(\infty) = 10$ is

   $$\tau = \tau_0 := \frac{1}{5\sqrt[3]{60}} \approx 0.0511.$$

   Note that the bandwidth of the resulted T_{ref}, calculated by solving $|T_{\text{ref}}(\text{j}\omega)|^2 = 1/(\tau_0^2\omega^2+1)^3 = 1/2$, is

   $$\omega_{\text{b}} = 5\sqrt[3]{60}\sqrt{2^{1/3}-1} \approx 9.98\,[\text{rad/sec}],$$

   which is about a half of the bandwidth of the complementary sensitivity system T.

   Simulation results for this system are presented in Fig. 8. Solid lines there represent frequency- and time-responses of the 2DOF controller in Fig. 7, dashed lines represent the corresponding responses in the unity-feedback setup. Comparing the plots in Fig. 8(a), we can see that the 2DOF design results in smoother frequency response from r to y. As a result, the step command response, which corresponds to the interval $[0, 1.84]$ in Fig. 8(b), is considerably smoother in the 2DOF case, it has no overshoot. Its settling time, under settling level 1%, is then about 0.43 [sec], which is shorter than that in the 1DOF case by more than a factor of 4, even though the bandwidth of T_{ref} is only a half of that of T. The disturbance responses, which start at $t = 1.84$ in Fig. 8(b), are identical in both cases because the response to d depends only on the controller C in the feedback loop (the plots slightly differ because they start from slightly different points). The control signal starts from the same amplitude $u(0) = 10$ in both cases, because we took care to have the same high-frequency gains of T_{ur} and T_{c}. But the 2DOF design yields a less oscillatory control trajectory for a step r (control trajectories in response to d are again identical in both designs).

3. We already know that the only constraint on $T_{\text{ref}}(s)$ is that its pole excess is ≥ 3. From

   $$C_{\text{ol}}(s) = \frac{T_{\text{ref}}(s)}{P(s)} = T_{\text{ref}}(s)\frac{s(s+5)(s+10)}{750}$$

   it should be clear that the degree of $C_{\text{ol}}(s)$ can be reduced if poles of $T_{\text{ref}}(s)$ are canceled by zeros. It should also be clear that only stable zeros may be canceled, because otherwise T_{ref} is not stable. This fixes two poles of $T_{\text{ref}}(s)$ to $s = -5$ and $s = -10$ and results in

   $$T_{\text{ref}}(s) = \frac{50}{(\tau s+1)(s+5)(s+10)}$$

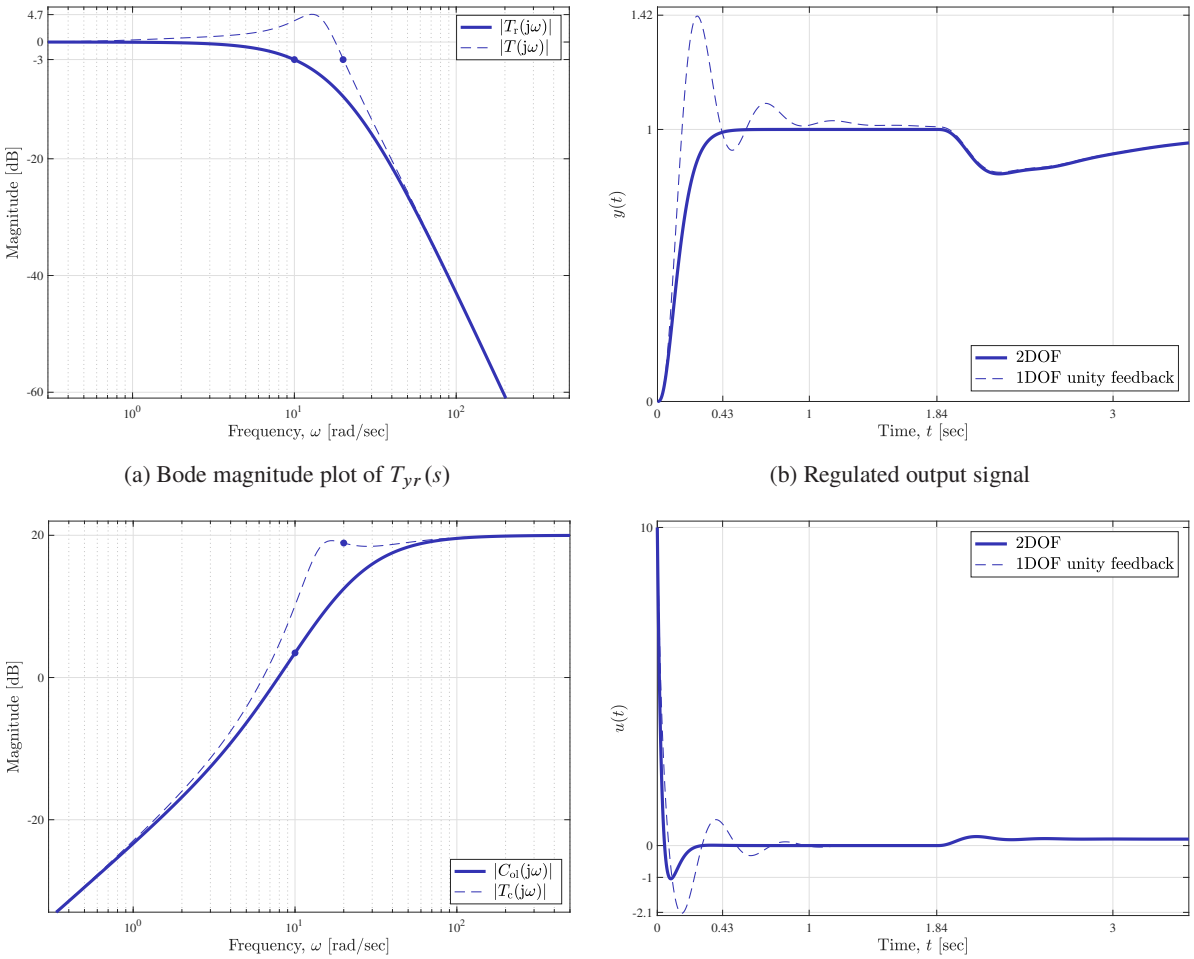

(a) Bode magnitude plot of $T_{yr}(s)$

(b) Regulated output signal

(c) Bode magnitude plot of $T_{ur}(s)$

(d) Control input signal

Fig. 8: Closed-loop responses for $T_{\text{ref}}(s) = 1/(\tau s + 1)^3$

(remember the static gain requirement) and the first-order

$$C_{\text{ol}}(s) = \frac{s}{15(\tau s + 1)}.$$

The time constant of C_{ol} is chosen from the requirement $C_{\text{ol}}(\infty) = 10$, leading to

$$\tau = \tau_1 = \frac{1}{150} \approx 0.00667.$$

The bandwidth of the resulted T_{ref}, calculated by solving $|T_{\text{ref}}(j\omega)|^2 = 1/2$ again, is

$$\omega_{\text{b}} \approx 4.1762\,[\text{rad/sec}],$$

which is more than twice smaller than in the previous design, in which the complexity of C_{ol} was not accounted for. We may thus expect that the resulting response is slower.

Simulation results for this system are presented in Fig. 9, with the same convention as in the previous item. Comparing the plots in Fig. 9(a), we can see that the 2DOF design again results in a smoother frequency response from r to y, because the stable poles of the transfer function $P(s)$

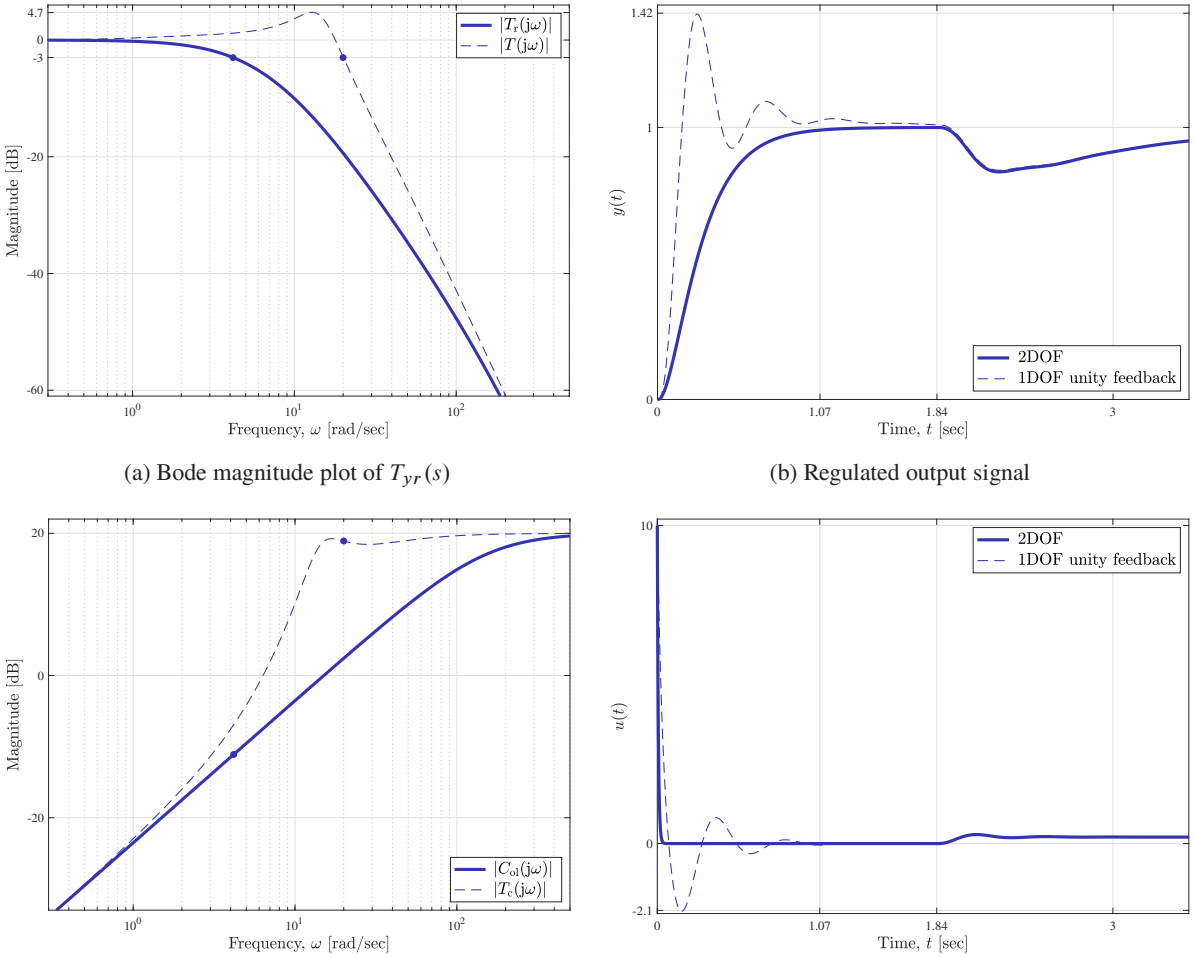

(a) Bode magnitude plot of $T_{yr}(s)$

(b) Regulated output signal

(c) Bode magnitude plot of $T_{ur}(s)$

(d) Control input signal

Fig. 9: Closed-loop responses for $T_{\text{ref}}(s) = 50/((\tau s + 1)(s + 5)(s + 10))$

of the plant in $T_{\text{ref}}(s)$ are real. As a result, the step command response, which corresponds to the interval $[0, 1.84]$ in Fig. 9(b), is considerably smoother in the 2DOF case, it has no overshoot. Its settling time, under settling level 1%, is now about 1.07 [sec], which is still slightly shorter than that in the 1DOF case, even though the bandwidth of T_{ref} is almost 5 times narrower that that of T (its bandwidth is 20 [rad/sec]). The disturbance responses, which start at $t = 1.84$ in Fig. 9(b), are again virtually indistinguishable in both cases, because the response to d depends only on the controller C in the feedback loop. The control signal, see Fig. 9(d), starts from the same amplitude $u(0) = 10$ in both cases, because we took care to have the same high-frequency gains of T_{ur} and T_c. But now the 2DOF design yields a substantially shorter and monotonically decreasing control trajectory for a step r. In fact, because the step response of a system with the transfer function $G(s)$ equals the impulse response of a system with the transfer function $G(s)/s$, the control signal is the impulse response of $1/(15(\tau_1 s + 1)) = 10/(s + 150)$, which satisfies $u(t) = 10\text{e}^{-150t}\,\mathbb{1}(t)$. This signal decays rapidly and effectively vanishes in 0.03 [sec].

The moral here is that 2DOF control configurations provide us with an efficient and easy-to-use tool to improve the command response without altering feedback properties (like the disturbance attenuation) of the system. ▽